Difference in Fractional Occurrences of Precipitation Categories in Terms of Cloud Properties

Kazuaki Kawamoto[a] and Kentaroh Suzuki[b]

[a]*Graduate School of Fisheries Science and Environmental Studies, Nagasaki University, 1-14 Bunkyo-mamachi, Nagasaki, Japan*
[b]*Jet Propulsion Laboratory, California Institute of Technology, 4800 Oak Grove Drive, Pasadena, CA 91109, USA*

Abstract. The relationship between the precipitation stage and water cloud properties was studied in the mid-latitudes using space-borne radar and radiometer data, with a focus on a comparison between continental (over China) and oceanic (over the northwest Pacific) clouds. More specifically, fractional occurrences of the precipitation categories were investigated in terms of two-dimensional representations of cloud parameters, such as combinations of optical depth – effective particle radius, and liquid water path - droplet number density. As a result, systematic changes in the transition regarding pairs of the cloud parameters were well captured for all precipitation categories. The transition pattern was similar for both land and oceanic clouds. Notably, the ranges of all values of cloud parameters (except cloud droplet number density) were considerably larger for oceanic clouds for the precipitating category.

Keywords: Clouds, Drizzle, Precipitation, Microphysical properties.
PACS: 92.60.Nv, 92.60.Vb

INTRODUCTION

Clouds play key roles in climate systems; for example, they produce precipitation and control the global energy budget via their effects on solar and infrared radiative transfer processes. It is important to understand the relationship between the precipitation stage and cloud physical properties such as optical depth (τ_c), effective particle radius (r_e), liquid water path (LWP) and droplet number density (N_c) for determining the effects of clouds on climate. Among various types of clouds in the Earth's atmosphere, water clouds occupy a large area of the atmosphere over both oceans and land and have been examined more extensively than ice clouds for several reasons. One reason is that in situ measurements are easier to conduct for water clouds, which occur in the lower atmosphere, than for high altitude ice clouds. Moreover, because water droplets are assumed to be spherical, Mie scattering theory can be applied to radiative transfer calculations. Conversely, it is difficult to determine the scattering properties of the nonspherical particles found in ice clouds.

Recently, active remote sensing data have become available, such as those from the CloudSat satellite. Launched in April 2006, CloudSat carries the Cloud Profiling Radar (CPR), operating at 94 GHz. A synergetic approach using both active and passive instruments, such as in the A-Train satellite constellation, is an extremely powerful tool in revealing the detailed vertical droplet structures inside clouds, which were previously unknown. A method that combines the radar reflectivity (Z_e) inside the cloud layer from CloudSat with the τ_c of the whole cloud layer, as well as r_e near the cloud top from Moderate Resolution Imaging Spectroradiometer (MODIS), has been devised and used by several previous studies [1-4]. In this study, we investigated the fractional occurrences of precipitation categories as a function of combinations of optical depth – effective particle radius, and liquid water path - droplet number density in the context of their two-dimensional representations.

DATA

This study used the following five cloud parameters: τ_c, r_e, LWP, N_c and Z_e. The τ_c and r_e data were retrieved from MODIS visible (non-absorbing) 0.6-μm and near-infrared (absorbing) 2.1-μm channels [5]. LWP and N_c values were derived from τ_c and r_e retrievals according to the adiabatic growth assumption: LWP was calculated as $5\tau_c r_e/9$ and N_c was estimated using equation (1) below originally from equation (3) of Kubar et al. [6]:

Radiation Processes in the Atmosphere and Ocean (IRS2012)
AIP Conf. Proc. 1531, 424-427 (2013); doi: 10.1063/1.4804797

$$N_c = \sqrt{2}\, B^3 \Gamma_{\mathrm{eff}}^{1/2} \mathrm{LWP}^{1/2} / r_e^3, \quad (1)$$

where $B = (3\pi\rho_w/4)^{1/3} = 0.0620$, ρ_w is the density of liquid water, and Γ_{eff} is the adiabatic rate of increase in the liquid water content with height. Γ_{eff} is weakly dependent on pressure and temperature and was derived from a diagram of Wood [7]. Z_e was obtained from the CloudSat 2B-GEOPROF product [8, 9]. Additionally, altitude and temperature profiles were obtained from the European Centre for Medium-Range Weather Forecasts Auxiliary (ECMWF-AUX) dataset matched to CloudSat radar footprint [10].

We used the above CloudSat data, collocated with MODIS products for the periods of June, July, and August (JJA) and December, January, and February (DJF) from 2006 to 2008, to examine the averaged behaviors of single-layered water clouds over these seasons in mid-latitudes. The two target areas are one over land (within 1000 km from 35°N and 105°W over China) and one over ocean (within 1000 km from 35°N and 165°E over the northwest Pacific) at mid-latitudes, which are specified in Figure 1. These regions were chosen because they are adjacent and nearly continuous over the same latitudes, and therefore are suitable for the comparison analysis of land-ocean contrasts in mid-latitude water (liquid-phase) clouds. In this study, we confine our analyses to low-level water clouds because of their large area of coverage and substantial radiative effect. To avoid the complexity that arises from multi-layered clouds, we selected only single-layered clouds. We adopted a method of Haynes and Stephens [11] for detection of the single-layered clouds.

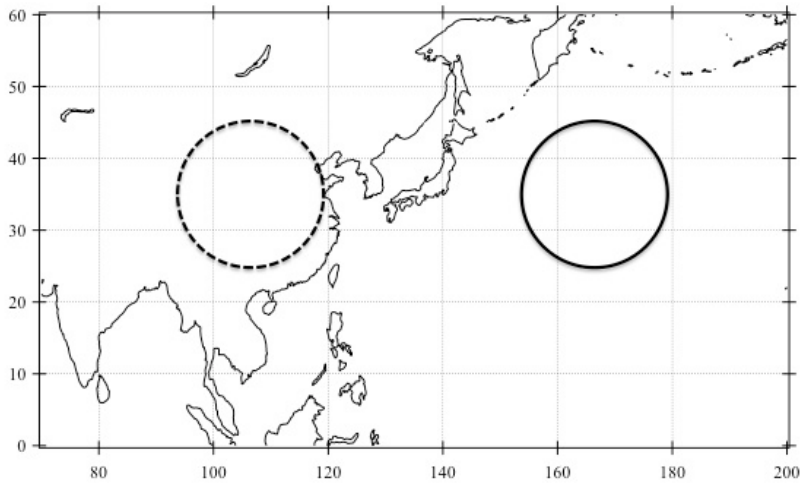

FIGURE 1. Map of the regions analyzed in this study. Dashed and solid circles represent the land areas (within 1000 km from 35°N and 105°W over China) and oceanic areas (within 1000 km of 35°N and 165°E over the NW Pacific), respectively.

RESULTS AND CONCLUSIONS

To achieve the purpose of this study, the following three precipitation categories were classified according to the maximum Z_e value within the cloud layer. The precipitation categories were defined with threshold values as follows: (i) non-precipitating ($Z_e < -15$ dBZ); (ii) drizzle (-15 dBZ $< Z_e < 0$ dBZ), and (iii) precipitating (0 dBZ $< Z_e$). The fractional occurrences of precipitation categories are investigated by the two-dimensional representations, according to the method of Suzuki et al. [12].

Figure 2 shows fractional occurrences of precipitation categories as a function of τ_c and r_e over land (upper panels) and ocean (lower panels). The overall behaviors of the contributions of τ_c–r_e to differences between non-precipitating and precipitation categories were similar for land and oceanic clouds. For example, the non-precipitating category generally occurs in the region of small τ_c with broad r_e values and small r_e with broad τ_c values. The drizzle category mainly appears over the intermediate region between larger τ_c and smaller r_e to smaller τ_c and larger r_e. The precipitating category occupies the remaining lower-right region having larger τ_c and r_e values. Nevertheless, the precipitation category displays greater differences between land and oceanic clouds

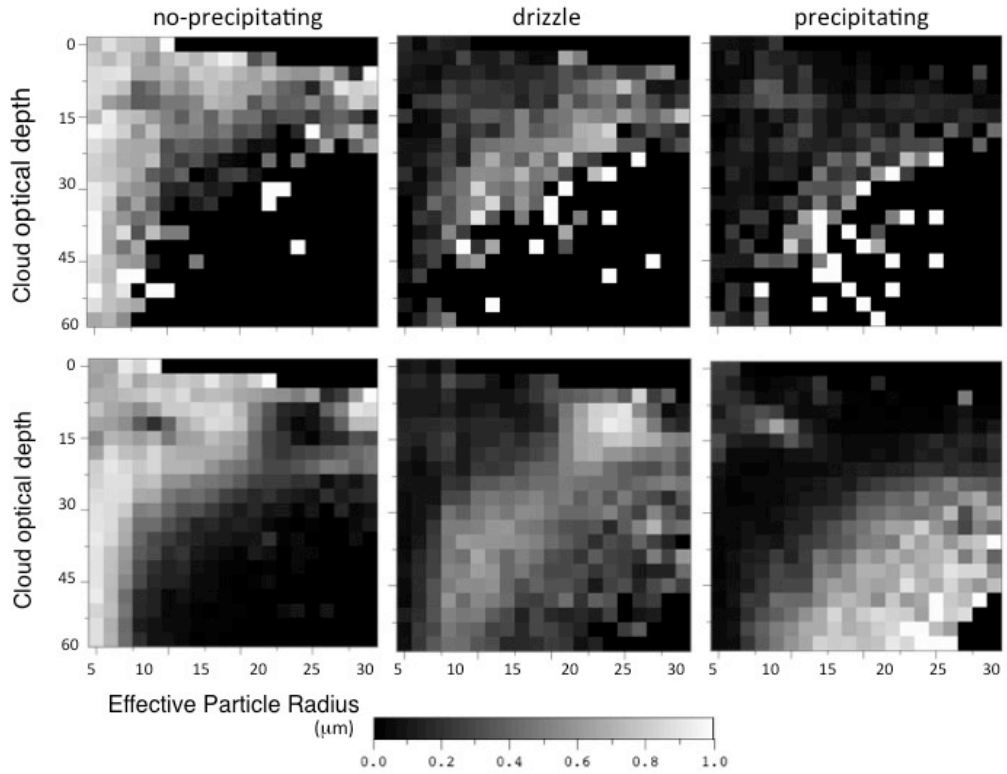

FIGURE 2. Fractional occurrences of non-precipitating, drizzle, and precipitation as a function of τ_c and r_e for land (upper panels) and oceanic (lower panels) clouds.

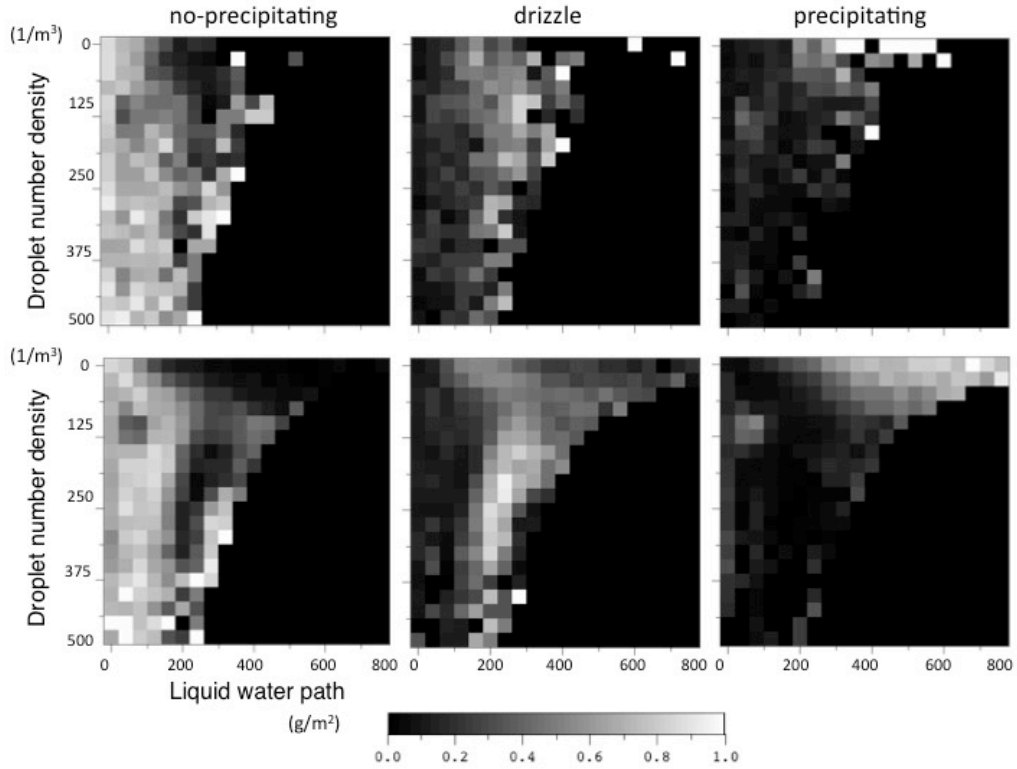

FIGURE 3. As in Figure 2, but as a function of LWP and N_c.

among non-precipitating, drizzle, and precipitating categories. As pointed out by Suzuki et al. [12], this approach can reveal how cloud properties contribute to each precipitation category, and how they tend to systematically vary among each precipitation category. When compared to the other categories, oceanic clouds show greater frequencies of the precipitating category over larger values of τ_c and r_e.

Figure 3 shows fractional occurrences of the precipitation categories as a function of LWP and N_c over land (upper panels) and ocean (lower panels). The non-precipitating category was shown to occur generally over small LWP with broad N_c values. The drizzle category was found to take place over larger LWP than the non-precipitating category. The precipitating category was shown to occur in the upper-right region of the N_c -LWP plane, corresponding to larger LWP and smaller N_c. As in the τ_c–r_e case, the precipitation characteristics in terms of the LWP–N_c plane are similar between land and oceanic clouds, although oceanic clouds have larger LWP values than land clouds. For both the τ_c–r_e and LWP–N_c cases, fractional frequencies of the precipitation categories are systematically shifted

Systematic changes in the transition regarding pairs of the cloud parameters were well captured for all precipitation categories. The transition pattern was similar for both land and oceanic clouds. Notably, the ranges of all values of cloud parameters (except N_c) were considerably larger for oceanic clouds for the precipitating category.

ACKNOWLEDGMENTS

K. Kawamoto was supported by the Mitsui & Co., Ltd., Environment Fund, Grant-in aid for Scientific Research (B) and Grant-in aid for Scientific Research on Innovative Areas. The CloudSat data products of 2B-GEOPROF and MODIS-AUX and ECMWF-AUX were provided by the CloudSat Data Processing Center at CIRA/Colorado State University. Part of the research was carried out at the Jet Propulsion Laboratory, California Institute of Technology, under a contract with the National Aeronautics and Space Administration.

REFERENCES

1. M. D. Lebsock, G. L. Stephens and C. Kummerow, *J. Geophys. Res.* **113**, D15205, doi:10.1029/2008JD009876 (2008).
2. T. Y. Nakajima, K. Suzuki and G. L. Stephens, *J. Atmos. Sci.* **67**, 1897–1907 (2010).
3. K. Suzuki, T. Y. Nakajima and G. L. Stephens, *J. Atmos. Sci.* **67**, 3019–3032 (2010).
4. K. Kawamoto and K. Suzuki, *J. Geophys. Res.* **117**, D05212, doi:10.1029/2011JD016412 (2012).
5. S. Platnick, M. D. King, S. A. Ackerman, W. P. Menzel, B. A. Baum, J. C. Riedi and R. A. Frey, *IEEE Trans. Geosci. Remote Sens.* **41**, 459–473, doi:10.1109/TGRS.2002.808301 (2003).
6. T. L. Kubar, D. L. Hartmann and R. Wood, *J. Atmos. Sci.* **66**, 2953–2972 (2009).
7. R. Wood, "Relationships between optical depth, liquid water path, droplet concentration, and effective radius in an adiabatic layer cloud," University of Washington, 3 pp. (2006). [Available online at http://www.atmos.washington.edu/~robwood/papers/chilean_plume/optical_depth_relations.pdf].
8. G. G. Mace, R. Marchand, Q. Zhang and G. L. Stephens, *Geophys. Res. Lett.* **34**, L09808, doi:10.1029/2006GL029017 (2007).
9. R. Marchand, G. G. Mace, T. Ackerman and G. L. Stephens, *J. Atmos. Ocean Tech.* **25**, 519–533 (2008).
10. P. Partain, "Cloudsat ECMWF-AUX auxiliary data process description and interface control document" CloudSat Project, CIRA, Colorado State University, Fort Collins (2007). [Available online at http://www.cloudsat.cira.colostate.edu/data ICDlist.php?go=list&path=/ECMWF-AUX].
11. J. M. Haynes and G. L. Stephens, *Geophys. Res. Lett.* **34**, L09811,doi:10.1029/2007GL029335 (2007).
12. K. Suzuki, G. L. Stephens, S. C. van den Heever and T. Y. Nakajima, *J. Atmos. Sci*. **68**, 2655-2670 (2011).